MAIN ROTOR - TAIL ROTOR WAKE INTERACTION AND ITS IMPLICATIONS FOR HELICOPTER DIRECTIONAL CONTROL

Timothy M. Fletcher[1], **Richard E. Brown**[2]

[1]Postgraduate Research Assistant
Department of Aeronautics
Imperial College
London, SW7 2AZ, United Kingdom
e-mail: timothy.fletcher@imperial.ac.uk

[2]Mechan Professor of Engineering
Department of Aerospace Engineering
University of Glasgow
Glasgow, G12 8QQ, United Kingdom
e-mail: rbrown@aero.gla.ac.uk

Key Words: Rotor Wake, Aerodynamic Interaction, Directional Control

Abstract. Aerodynamic interference between the main and tail rotor can have a strong negative influence on the flight mechanics of a conventional helicopter. Significant unsteadiness in the tail rotor loading is encountered under certain flight conditions, but the character of the unsteadiness can depend on the direction of rotation of the tail rotor. Numerical simulations, using Brown's Vorticity Transport Model, of the aerodynamic interaction between the main and tail rotors of an idealised helicopter are presented for a range of forward and lateral flight speeds. Distinct differences are predicted in the behaviour of the system in left and right sidewards flight that are consistent with flight experience that the greatest fluctuations in loading or control input are required in left sideways flight (for a counter-clockwise rotating rotor) and are generally more extreme for a system with tail rotor rotating top-forward than top-aft. Differences are also exposed in the character of the lateral excitation of the system as forward flight speed is varied. The observed behaviour appears to originate in the disruption of the tail rotor wake by entrainment into the wake of the main rotor. The extent of the disruption is dependent on flight condition, and the unsteadiness of the process depends on the direction of rotation of the tail rotor. In high-speed forward flight and right sidewards flight, the free stream delays the entrainment to far enough downstream for the perturbations to the rotor loading to be slight. Conversely, in left sidewards and quartering flight, the free stream confines the entrainment process close to the rotors where it causes significant unsteadiness in the loads produced by the system.[3]

[3]Presented at the 32nd European Rotorcraft Forum, Maastricht, Netherlands, 2006.

NOMENCLATURE

N	airframe yaw moment	μ	overall advance ratio, $(\mu_x^2+\mu_y^2)^{1/2}$
N_{mr}	main rotor contribution to yaw moment	Ω	main rotor speed
N_{tr}	tail rotor contribution to yaw moment	S	vorticity source
$C_{T_{tr}}$	tail rotor thrust coefficient	u	flow velocity
θ_0	main rotor collective pitch	u_b	flow velocity relative to blade
$\theta_{0_{tr}}$	tail rotor collective pitch	ω	vorticity
θ_{1s}	main rotor longitudinal cyclic pitch	ω_b	bound vorticity
θ_{1c}	main rotor lateral cyclic pitch	ν	kinematic viscosity
F^*	target airframe forces and moments	i	sample index
F	current airframe forces and moments	Δt	time interval
τ	matrix of time constants		
R	main rotor radius	**notation:**	
R_t	tail rotor radius	$\bar{x}$	time-averaged value of x(t)
μ_x	advance ratio in x-direction	x'	perturbation of x(t) from time-average
μ_y	advance ratio in y-direction	$\hat{x}$	RMS value of x(t)

1 INTRODUCTION

The need to correct or rectify the effects of aerodynamic interactions that were unforseen or mis-predicted at the design stage has historically been one of the most common causes of delay in the advancement of a new helicopter design from prototype to production. Interference between the wakes and other flow disturbances induced by the helicopter's rotors, fuselage and lifting surfaces can produce strong loads on geometrically distant parts of the configuration. Any unsteadiness in these loads, or change in these loads as the flight condition of the aircraft is altered, can have a very strong negative influence on the dynamics of the vehicle. Experience within the helicopter industry suggests that the nature and form of the aerodynamic interactions that arise from even minor configurational changes to an airframe can be extremely difficult to predict, and this lack of predictive capability attaches a significant degree of risk to any departures from established design practice.

In a conventionally configured helicopter, a single, large main rotor provides propulsion and lift, while a smaller tail rotor, mounted behind the main rotor, is oriented transversely to the main rotor to provide a counter-torque reaction to the fuselage. This paper will focus on a particularly poorly understood element of the interactional aerodynamic environment of this configuration, namely the effect on the performance of the tail rotor of its operation in close proximity to the flow field of the main rotor. The interaction of the main rotor wake with that of the tail rotor, and more directly, it's impingement on the tail rotor itself, adds both unsteadiness and nonlinearity to the performance of the tail rotor.

In 1980, Sheridan and Smith[1] produced an authoritative survey of the various known aerodynamic interactions within the helicopter system and, in the interests of drawing the community's attention to the many and varied forms that aerodynamic interactions within the helicopter system could take, categorised these according to the aircraft components involved in the interaction (e.g. ‘main rotor - fuselage’ or ‘main rotor - tail rotor’) and the associated flow anomaly (e.g. ‘flow redirection’, ‘flow field distortion’ or ‘wake impingement’) responsible for the observed dynamic effects on the system. Indeed, Sheridan and Smith noted that thrust distortion and an increased power requirement, compared to the same rotors tested in isolation, were specific problems associated with main rotor - tail rotor interaction. Interestingly, Sheridan and Smith also categorised main rotor - tail rotor and tail rotor - main rotor interactions separately, acknowledging the effects of mutual interference on the performance of both components.

An important design parameter, from a handling qualities perspective at least, appears to be the sense of rotation of the tail rotor. The tail rotor of a conventional helicopter can be classified as having either top-aft (TA) or top-forward (TF) sense of rotation, implying that its blades travel respectively rearward or forward at the top of the disc. Helicopter designers often refer to a ‘right way’ and a ‘wrong way’ for the tail rotor to rotate. The overview of tail rotor design published by Lynn *et al.*[2] in 1970 described clear differences in performance for systems with TA and TF rotation, but also acknowledged the obscurity of the aerodynamic origins of these differences. The differences in performance between systems equipped with TA and TF rotating tail rotors seem to manifest themselves most clearly in sideways flight as a large increase in the pedal activity required to trim the aircraft in yaw (usually for the system with TF tail rotor rotation) with one direction of flight generally being more affected than the other. Yet the number of helicopters in the last few decades that have progressed through the design process, only to have the direction of rotation of their tail rotors reversed during full-scale development, testifies to a continued lack of understanding of the detailed reasons why the direction of tail rotor rotation should have such a marked effect on aircraft performance. Notable works describing situations where the sense of rotation of the tail rotor became a significant issue in the design of the aircraft include the study of the AH-56A Cheyenne by Johnston and Cook[3], the YAH-64 Apache by Amer *et al.*[4] and Prouty[5] and the wind-tunnel tests by Yeager *et al.*[6] Indeed, it is likely that the tail shake phenomenon[7], which has emerged during flight test of several helicopters, is also exacerbated by main rotor - tail rotor aerodynamic interaction and is influenced, to some extent, by the direction of rotation of the tail rotor.

Unfortunately, most published experimental research on main rotor - tail rotor aerodynamic interaction has been performed on configurations where it has been difficult to isolate the specific effects of the aerodynamic interaction between the main and tail rotors on the performance of the system. Inferences from the influential data set obtained by Balch[8], for instance, are obscured by the presence of a fuselage in the experimental set-up. The works of Empey and Ormiston[9] and Wiesner and Kohler[10] were both valuable contributions to the field, but interpretation of both studies is complicated by the presence of strong ground effect. The highly suggestive, but unpublished, small-scale experiments on isolated rotors in hover by Brocklehurst[11] must be cited as a major inspiration to the present work, however.

Although much remains to be achieved, numerical helicopter models, particularly those using computational fluid dynamics (CFD) techniques to capture the structure and form of the wakes induced by helicopter rotors, have advanced to the point where the potential exists to model some aspects of the aerodynamic interactions between the various components of the helicopter to an appreciable degree of realism. The present work uses such a model to examine the flow physics that underly the aerodynamic interaction between the main and tail rotors of the conventional helicopter configuration, and in particular to investigate some of the differences in aerodynamic behaviour of the system that result from a change in the sense of rotation of the tail rotor. The advantage of the computational approach is that, unlike in the laboratory or in full-scale flight test, complicating factors such as the presence of ground effect, and the uncertainty in interpretation of results that is introduced by the presence of secondary aerodynamic interference from fuselage and fins, can be eliminated very easily, revealing the fundamental processes at work.

2 HELICOPTER MODEL

The performance of a generic conventional helicopter configuration has been simulated using the Vorticity Transport Model (VTM) developed by Brown[12], and extended by Brown and Line[13]. The VTM is a comprehensive rotorcraft model in which the flow field around the rotorcraft is obtained by solving the time-dependent Navier-Stokes equation, in finite-volume form, on a structured Cartesian mesh enclosing the helicopter system. The key to the VTM is its use of the vorticity-velocity form of the incompressible Navier-Stokes equation,

$$\frac{\partial}{\partial t}\omega + u \cdot \nabla\omega - \omega \cdot \nabla u = S + \nu\nabla^2\omega \tag{1}$$

that relates the evolution of the vorticity field ω, representing the wake, to the velocity field u. The source term

$$S = -\frac{d}{dt}\omega_b + u_b\nabla \cdot \omega_b \tag{2}$$

accounts for the production of vorticity in the flow as a result of spatial and temporal changes in the bound vorticity distribution ω_b on the various lifting surfaces of the rotorcraft. This system of equations is closed by relating the velocity to the vorticity using the Biot-Savart relationship

$$\nabla^2 u = -\nabla \times \omega \tag{3}$$

which is solved in the VTM using a Cartesian fast multipole method. Numerical diffusion of the vorticity in the flow-field surrounding the rotorcraft is kept at a very low level by using a Riemann problem based technique based on Toro's Weighted Average Flux method[14] to advance Eq. 1 through time. This approach allows highly efficient multi-rotor simulations, and permits many rotor revolutions to be captured without significant dissipation of the wake structure, in contrast to the performance of more conventional CFD techniques based on the pressure-velocity formulation of the Navier-Stokes equation. Hence, in principle, both the low (1/rev and lower) frequency components of the loading which influence the body dynamics but are often the result of the dynamics of large-scale structures in the flow, and the high frequency (1/rev and higher) components which are important for the dynamic response of the rotors but are generally governed by smaller-scale flow features such as blade-vortex interactions, can be resolved simultaneously within the same computation. The VTM has been used previously for helicopter flight mechanics research by Brown and Houston[15], and Houston and Brown[16], and for the investigation of the interaction of helicopters with aircraft wakes by Whitehouse and Brown[17] and the rotor vortex ring state by Brown *et al.*[18].

In this study, the helicopter is represented simply as a pair of rotors, oriented in conventional fashion with their centres located at representative points in the flow. This idealisation of the problem ensures that solely the effects of the interactions between the rotors are captured, uncomplicated by the presence of further aerodynamic interactions betwen rotors and fuselage or fins. The principal parameters for the main and tail rotors are given in Tables 1 and 2 respectively, and the relative locations of the main and tail rotors are shown in Fig. 1. The main rotor rotates anti-clockwise when viewed from above, hence the tail rotor produces a force to the right in trimmed flight.

Table 1: Main Rotor Data

No. of blades	3
Rotor radius	R
Chord	$0.055R$
Twist	-8^o (linear)
Aerofoil	NACA 0012
Root cut-out	$0.19R$
Rotational speed	Ω

Table 2: Tail Rotor Data

No. of blades	3
Rotor radius	$R_t = 0.193R$
Chord	$0.186R_t$
Twist	0^o
Aerofoil	NACA 0012
Root cut-out	$0.21R_t$
Rotational speed	5.25Ω

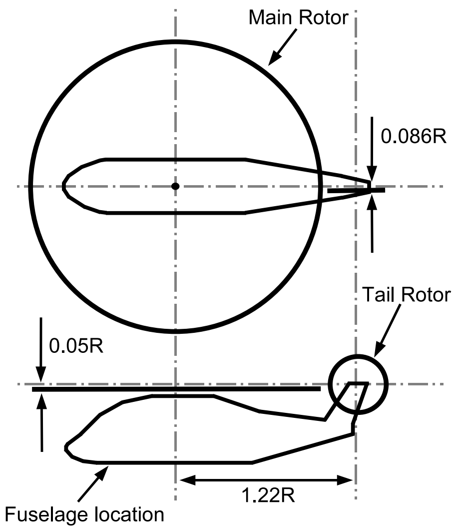

Figure 1: Rotor configuration (fuselage represented for clarity)

In all calculations, the rigid-body modes of the airframe were suppressed, yielding the computational equivalent of a model mounted rigidly in the test section of a wind-tunnel. This was done to simplify the analysis by eliminating feedback from the rigid-body modes into the aerodynamic loads generated on the rotors. In each simulation, the tail rotor collective pitch was controlled to ensure a zero net yaw moment on the rotorcraft. To eliminate as much complication from the analysis as possible, the longitudinal and lateral main rotor cyclic pitch was controlled to satisfy a very simplified trim condition of zero tilt of the main rotor disc, measured with respect to its shaft. The trim algorithm used within the calculations was a simple first-order scheme in which the instantaneous rate of change of the vector of controls, $u = (\theta_0, \theta_{1s}, \theta_{1c}, \theta_{0tr})$, is taken to be proportional to the error between a vector F, comprised of the forces, moments and disc-tilt angles that are to be controlled, and a vector of specified target values F^*:

$$\tau \frac{du}{dt} = F^* - F(t) \tag{4}$$

where τ is a suitably-defined matrix of time constants. Use of this controller yields an element of subjectivity in any measurements of control activity, since the results are affected by the particular choice of the elements of τ. These elements were thus set to prevent significant control input at frequencies much above 0.2-0.4 per main rotor revolution (as shown in Fig. 2), and hence to be roughly representative of the capabilities of a human pilot. Note though that this approach to the control of the helicopter needs to be tempered by the fact that, in handling qualities terms, the pilot is able to apply control inputs with a variety of different levels of aggression, the actual level depending on the task at hand. In general, the pilot will compromise on a certain degree of variability in the trajectory of the aircraft in exchange for a relaxation in required control activity. The results presented here thus fit within a broader spectrum of data that might be obtained by considering a more complete range of pilot attributes.

If the dynamics of the system is to be captured convincingly across the entire frequency spectrum of interest, then each simulation needs to be run for a very large number of rotor revolutions. The effort required to capture especially the low-frequency dynamics of the system results in simulations that are particularly demanding in terms of both memory and computational time. Thus, it is important to find a practical balance between computational effort and adequate resolution of the physical effects of importance in the situation being modelled. Fig. 2 shows part of the Fourier spectrum of the variation of tail rotor collective required to trim the helicopter in yaw in a series of test computations with the flow around the rotors resolved by grids with various cell sizes. The quartering flight case, described later in this paper, was used in these tests as it was found that this flight condition resulted in significant fluctuations in the tail rotor collective pitch required to maintain yaw moment equilibrium of the system. The figure shows that a certain minimum resolution of the aerodynamic features in the wake is required for these low-frequency fluctuations to emerge in the simulation. More importantly, the figure shows the simulated control response of the tail rotor to become relatively insensitive to the resolution of the flow once the cell size is reduced to about a twentieth of the main rotor radius. For this reason, all calculations presented in this paper were performed at this level of resolution. Note though that at this grid resolution the diameter of tail rotor is resolved over only about eight computational cells, and this does place a lower limit on the spatial dimensions of any interactional effects present in the simulation that can be fully resolved on the scale of the tail rotor. For instance, individual blade-vortex interactions at the tail rotor are not well captured at this level of resolution. Small-scale effects such as this would appear as high-frequency loads that would have to be properly resolved for accurate calculations of the acoustic or vibrational consequences of main rotor - tail rotor interactions, for instance, but the results presented here show that, given the characteristics of the controller, it is not really necessary to capture the aerodynamic environment of the tail rotor to the same level of detail in a study of the flight mechanics of main rotor - tail rotor interaction.

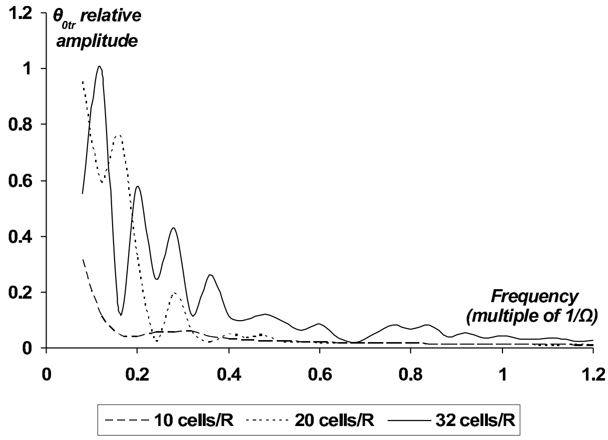

Figure 2: Sensitivity of tail rotor control response to grid resolution

3 THE EFFECTS OF AERODYNAMIC INTERACTION

Comparison of the results of simulations of the coupled main rotor - tail rotor system with the results of simulations of the same rotors in isolation shows the aerodynamic interaction between the wakes of the two rotors, when operated in close proximity to each other, to have a significant effect on the loads produced on both rotors. The interaction is characterised in particular by a marked increase in the unsteadiness of the loading on the system. This unsteadiness has important consequences for the flight mechanics and handling qualities of the helicopter. Data for seven different flight conditions is presented in this paper and results for simulations with both possible senses of tail rotor rotation are compared. As well as for hover, results are presented for two different forward flight speeds to determine the influence on the tail rotor performance of the rearwards skewing of the main rotor wake, and the possibility, over a range of flight speeds, of direct impingement of the main rotor wake on the tail rotor. Left-rearwards quartering flight was also examined to determine the effects on tail rotor performance of the relatively long-range interaction between the tail rotor wake and the developing super-vortices in the wake of the main rotor. Left and right sidewards flight at constant velocity was also considered. In this case the super-vortices formed in the wake of the main rotor do indeed pass very close to the tail rotor and influence very strongly its aerodynamic environment. Finally, results from a simulation of accelerated sidewards flight to the left are presented. In this example, the tail rotor is exposed to the possible onset of the vortex ring state over a range of flight speeds, and the possibility is that the behaviour of the tail rotor, once having succumbed to the instability of its wake and entered the vortex ring state, might be exacerbated by the proximity of the wake of the main rotor. To allow direct comparison between the various cases, the thrust coefficient of the main rotor was maintained at a nominal value of 0.005 throughout. The high-speed forward flight simulation was conducted at an advance ratio of 0.16, but, again to aid in their comparison, in all other cases except for the last, the overall advance ratio was kept constant at 0.04 and the flight condition was varied simply by flying the helicopter at the appropriate angle of sideslip.

Although the flight condition as well as the sense of rotation of the tail rotor has a strong influence on the actual performance of the system, the following example serves to illustrate the generic features of the interaction between the main and tail rotors before the results from the simulations of this broader series of flight conditions are presented and compared. Figs. 3(a)-3(d) show snapshots of the flow surrounding the helicopter when operated in hover. The structure of the rotor wakes is visualised in these diagrams by plotting a surface on which the vorticity in the flow surrounding the rotor has uniform magnitude. The selected vorticity magnitude is low enough for the global structure of the wake to be clearly apparent. Fig. 3(a) shows the wake of the isolated main rotor, and Fig. 3(b) the wake of the isolated tail rotor. When operated in isolation, both rotors generate a well-developed, cylindrical wake tube that extends some distance into the flow downstream of the rotor before succumbing to the natural instability of the wake tube to perturbations to the helicoidal geometry of its constituent vortex filaments. Figs. 3(c) and 3(d) show similar snapshots of the combined wakes of the main rotor and tail rotor when operated together, for the two cases where the tail rotor has TA and TF sense of rotation respectively. When influenced by the flow field of the main rotor wake, the tail rotor wake undergoes a radical change in its geometry. Instead of streaming out to the left of the helicopter as in the earlier image, after a very short distance it becomes entrained into the wake structure of the main rotor. Although the snapshots show the wake structures generated by the two systems with opposing sense of tail rotor rotation to be superficially very similar, this format of presentation does not represent very well the unsteadiness of the process by which the wakes of the two rotors merge. This is done more effectively by decomposing the vorticity in the wake into a mean component and an associated RMS fluctuation about the mean. The mean vorticity distribution is approximated simply as the ensemble average

$$\bar{\omega}(x,t) = \frac{1}{2n+1} \sum_{i=-n}^{n} \omega(x, t + i\,\Delta t) \qquad (5)$$

over $2n+1$ snapshots of the wake structure spaced apart by equal time intervals Δt. The associated RMS field representing the local fluctuations in the wake structure can then be calculated as

$$\hat{\omega}(x,t) = \left[\frac{1}{2n+1} \sum_{i=-n}^{n} \left(\omega(x, t + i\,\Delta t) - \bar{\omega}(t) \right)^2 \right]^{1/2} \qquad (6)$$

Fig. 4 shows the results of decomposing the flow into a persistent mean component (light, translucent surface) and a fluctuating RMS component (dark surface) using Eqs. 5 and 6. The development of the instability in the wake tube of both the isolated main and tail rotors is exposed very clearly in this form of presentation as a rather sudden increase in the fluctuating component of the vorticity, at the expense of the mean component, some distance downstream of both rotors. The effects of the interaction between the main and tail rotors, both in terms of the distortion of the shape of the mean wake and in the redistribution of the regions of maximum unsteadiness in the wake, is also clearly apparent in the two diagrams showing the flow field of the coupled system.

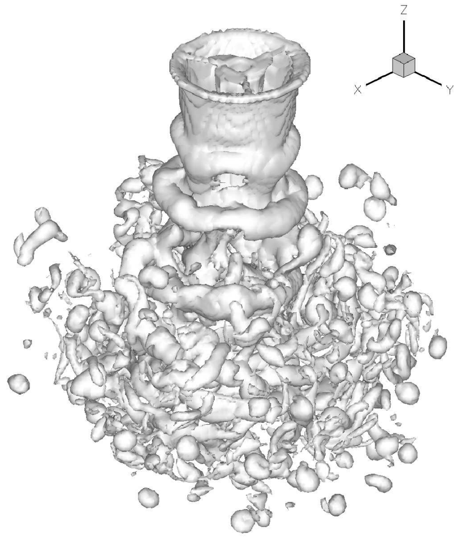

(a) Isolated main rotor

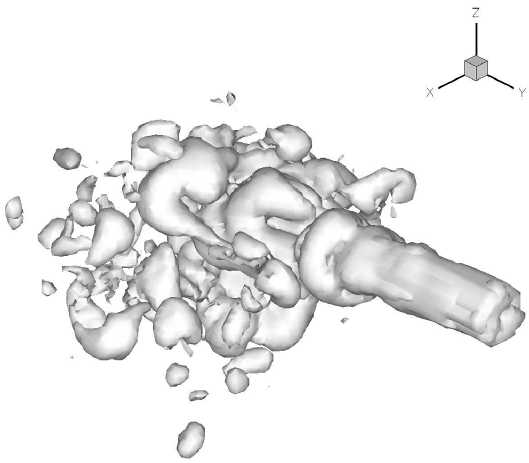

(b) Isolated tail rotor

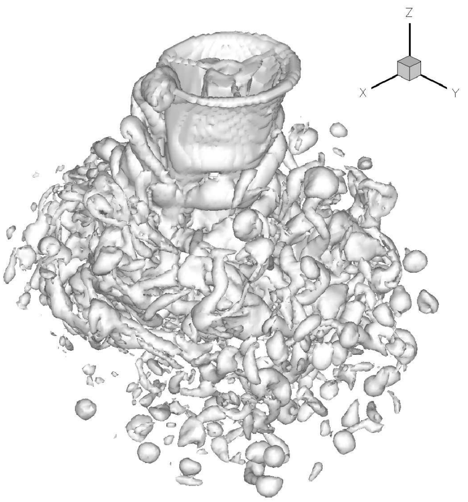

(c) Combined system, tail rotor top-aft

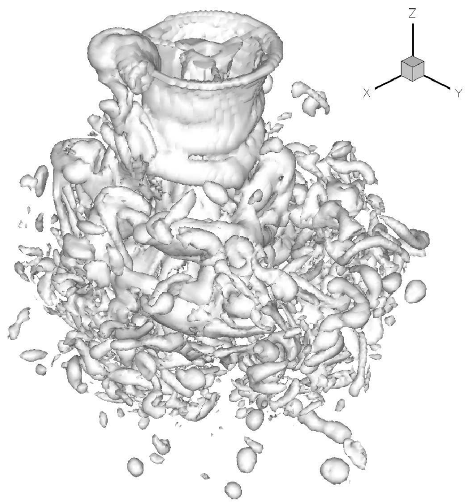

(d) Combined system, tail rotor top-forward

Figure 3: Instantaneous snapshots of hover wake

The systems with opposing directions of tail rotor rotation show not only distinct differences in mean wake geometry, especially in the region affected by the entrainment of the tail rotor wake into the wake-tube of the main rotor, but also in the distribution of the unsteadiness in the flow fields. Interaction with the main rotor wake causes the region of significant unsteadiness in what remains of the distinct wake tube of the tail rotor, if anything, to shrink when the tail rotor rotates TA, and the rather sparse distribution of the fluctuating component of the vorticity in this part of the wake suggests the relative steadiness of the entrainment process in this case. In contrast, when the tail rotor rotates TF, the fluctuating component of the vorticity is strongly concentrated in the region of the confluence of the two wake tubes, indicating that the entrainment process is accompanied by significant variability in the geometry of the wake. The extent to which the wake of the main rotor is affected by the interaction also appears to be quite strongly influenced by the direction of rotation of the tail rotor. With the tail rotor rotating TA, a reasonably narrow tongue of unsteadiness is introduced that extends down from the plane of the main rotor into the flow just to the left of the tail rotor. With the tail rotor rotating in the opposite sense, the region of unsteadiness that is induced in the main rotor wake by the interaction with the tail rotor is much larger, and extends to much of the aft left quadrant of the wake tube.

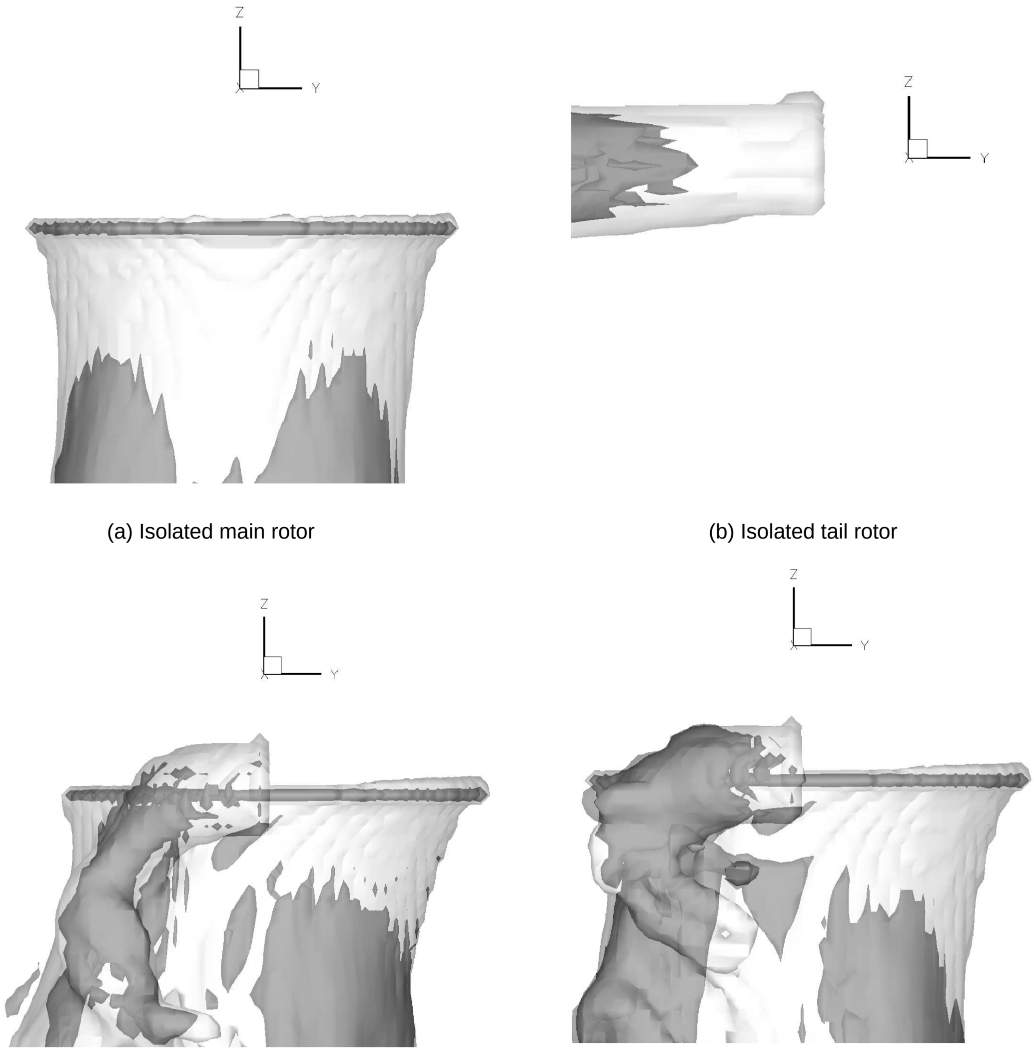

(a) Isolated main rotor

(b) Isolated tail rotor

(c) Combined system, tail rotor top-aft

(d) Combined system, tail rotor top-forward

Figure 4: Decomposition of hover wake into persistent and fluctuating components

The positions of these regions of unsteadiness in the flow appear to have a strong, but often quite obscure, influence on the loading produced on the system. As an example, Fig. 5 illustrates the unsteadiness in the thrust produced on the tail rotor, for both senses of tail rotor rotation, that is observed in a simulation of low-speed forward flight. This fluctuation in tail rotor thrust yields an unsteady contribution to the yaw moment on the vehicle, as does, in certain flight conditions, a similar fluctuation in the torque produced by the main rotor.

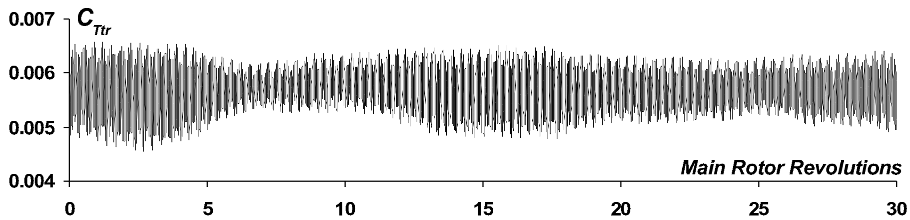

(a) Tail rotor top-aft

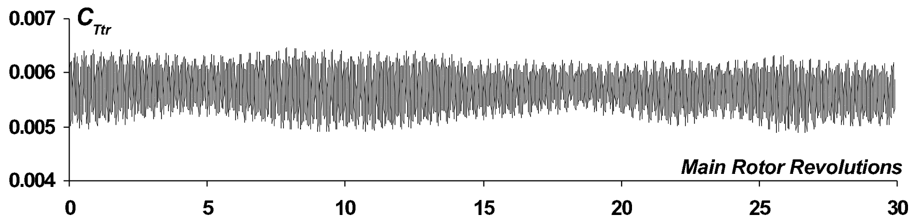

(b) Tail rotor top-forward

Figure 5: Tail rotor thrust coefficient in low-speed forward flight

4 ROTOR PERFORMANCE

If the unsteady yaw moment is required to be counteracted by the control system, then the aerodynamic unsteadiness associated with the interaction between the main and tail rotor wakes results in a fluctuation in the tail rotor collective pitch input. Fig. 6 shows the actions of the controller in attempting to drive the yaw moment to zero in six of the different flight conditions mentioned earlier, namely hover, level forward flight at low and high speed, left quartering flight, and left and right sideways flight. In each case, data is presented for both senses of tail rotor rotation. The data shown is for a sample extracted far enough into the simulation for the controller to have trimmed the system to a quasi-steady flight condition. In all cases there appears to be very little obvious periodicity in the control inputs required to trim the helicopter, but their low-frequency character is clearly apparent. It is clear too that the flight condition has a profound effect on the control activity required to maintain the aircraft in trim. Figs. 6(b) and 6(d) show that significant control activity is required to trim in quartering and left sideways flight and, to a lesser degree, also in low-speed forward flight as shown in Fig. 6(c). In contrast, little or no variation in tail rotor collective pitch is required to maintain trim in hover and high-speed forward flight, as shown in Figs. 6(a) and 6(e). Most interesting though is that in right sideways flight, as shown in Fig. 6(f), significantly less control activity is required to maintain trim than in the equivalent left sideways flight condition.

A very effective representation of the resultant loading fluctuations in the system is obtained by sampling the data at a fixed frequency (in this paper, unless otherwise stated, at once per main rotor revolution to expose the low-frequency unsteadiness in the signal that is of most relevance to the handling qualities of the aircraft) and projecting the sampled data back onto the real line to suppress the time axis. This representation of the data can be extended to multiple, concurrent time-series simply by increasing the number of axes in the plot. A series of such ‘return maps’, comparing the torque contributions from the main and tail rotors, is shown in Fig. 7 for the various flight cases considered in this paper. The scatter of points along each axis provides a measure of the variability in the associated time series, while clusters of points sometimes provide evidence of periodicity in the signal at sub-harmonics of the sampling frequency. Obvious structure in the distribution of points on the return map (although not an issue in the data presented here!) can sometimes be a sign that the system is governed by low-order dynamics, but such an interpretation needs to be made with care since the consequences are profound.

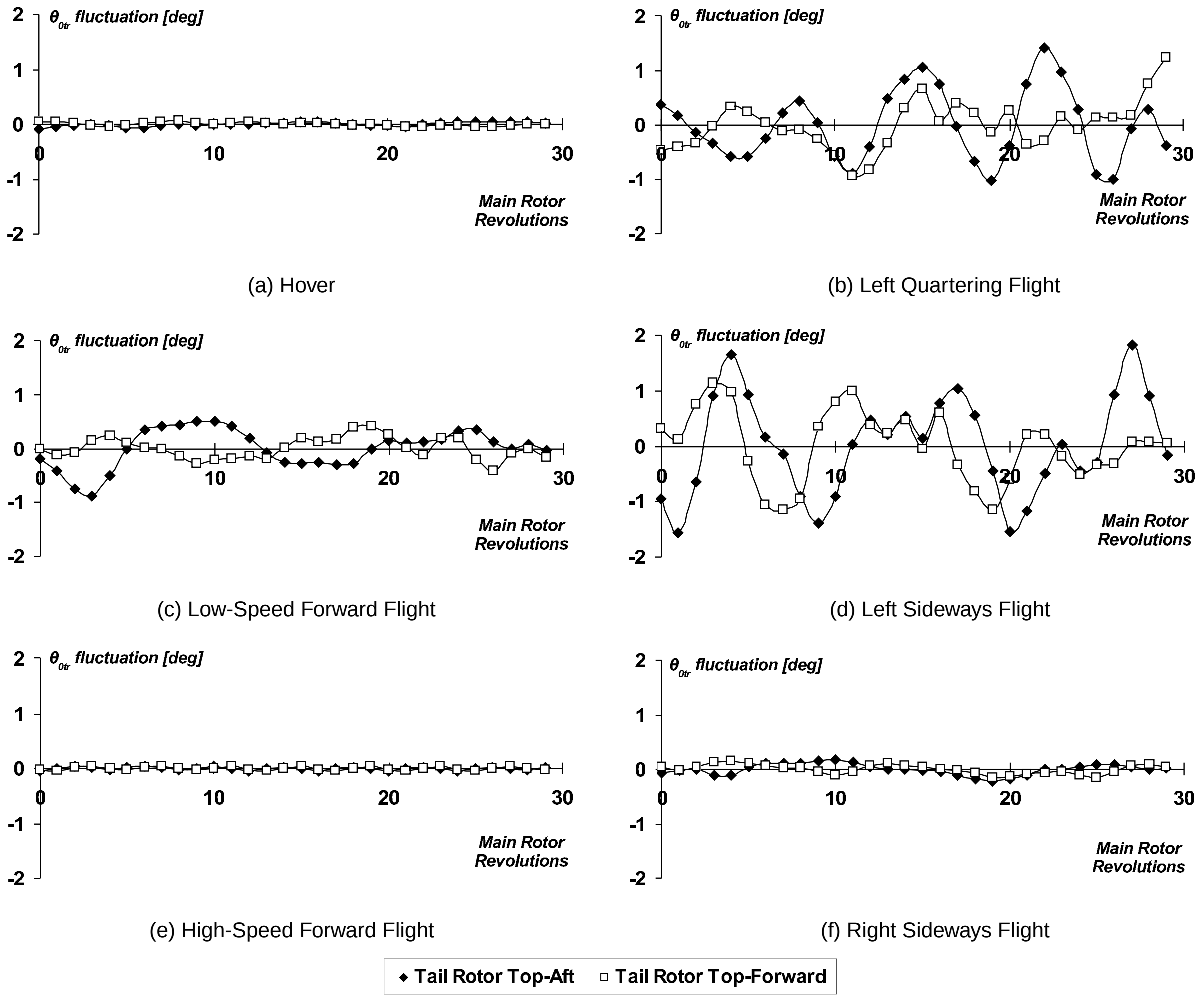

Figure 6: Variation in tail rotor collective pitch required for trim in yaw

To aid comparison between the different flight cases, the horizontal and vertical axes in Fig. 7 have both been scaled to represent the ratio of the fluctuation in the yaw moment contribution of each rotor to the mean value of the torque required by the main rotor in hover at the same thrust coefficient. The diagonal line on the diagrams thus represents the condition in which the net torque on the system is zero. It is clearly evident that the system spends very little time in this condition, and the degree of scatter in the distribution of data points around this line is representative of the magnitude of the fluctuation in torque about equilibrium. The degree of horizontal scatter of the data compared to the amount of vertical scatter is a measure of the relative contributions of fluctuations in tail rotor thrust and in main rotor torque to the lack of equilibrium within the system.

This form of presentation of the data reveals the main source of interaction-induced unsteady loading in the system to depend quite significantly on the flight condition: in hover and both low-speed and high-speed forward flight, the fluctuations in the thrust produced by the tail rotor are the most significant contributor, suggesting the dominance of the main rotor influence on the tail rotor in driving the interaction between the two rotors in forward flight. Most interestingly, the fluctuations in the tail rotor load are greater in the low-speed case than in the high, suggesting the existence of an intermediate advance ratio at which the aerodynamic interaction between the main and tail rotor has the most severe consequences for the handling qualities of the vehicle. The bimodal clustering of points in the return map for the low-speed case is also evidence for the existence of a very low-frequency periodicity in the forcing of the tail rotor that is not seen in any of the other flight conditions. This periodicity appears to be a slightly more prominent feature of the loading on the system with TF sense of tail rotor rotation than with TA, but besides this feature, the direction of tail rotor rotation appears to have very little influence on the behaviour of the system in forward flight.

In quartering and sideways flight, the interaction has a somewhat different character. The fluctuations in torque, although still dominated by the contribution from the tail rotor, arise partially also from the main rotor, suggesting the greater influence of the mutual interaction between the rotors on the dynamics of the system. In sideways flight to the right, both rotors yield relatively moderate contributions to the fluctuating torque on the system, and the behaviour of the system is relatively insensitive to the direction of tail rotor rotation. In sideways flight to the left, the system with TF sense of tail rotor rotation shows significantly elevated fluctuations in yaw moment compared to the system with TA-rotating tail rotor, and the contribution to the torque fluctuation from both rotors is significantly more extreme than in sideways flight to the right. The quartering flight case shows a slight elevation in the level of torque fluctuation compared to left sideways flight, and an even greater sensitivity to the direction of tail rotor rotation. Interestingly, the change from TA to TF sense of rotation results in an increase in the torque fluctuations generated by both the main and the tail rotors, rather than, as might be expected if the change in the sense of rotation had a more localised effect on the aerodynamics of the system, just in the torque fluctuation generated by the tail rotor. Despite the rather crude resolution of the aerodynamics of the tail rotor in these simulations, this observation is reasonably strong evidence that the origin of at least part of the sensitivity of the system's dynamics to the sense of rotation of the tail rotor lies in the mutual interference between the wakes generated by the two rotors rather than, as has been suggested in the past, being simply a function of the way that the tail rotor interacts locally with the wake of the main rotor.

It is possible that, at the particular advance ratio at which the simulations were conducted, both the left sideways flight case and, to a lesser degree, the quartering flight case may have involved the tail rotor operating in the vortex ring state (VRS). Fig. 8 shows the predicted tail rotor collective pitch variation required to trim the helicopter in yaw during a flight where the aircraft accelerates from hover into left sideways flight (with the tail rotor rotating TA). The negative trend of the tail rotor collective pitch with increasing lateral flight speed remains relatively stable up to a sideways advance ratio of approximately 0.02. For advance ratios between 0.02 and 0.04, though, the obvious increase in tail rotor collective pitch required to trim the aircraft is very similar in character to the thrust settling and onset of the vortex ring state that would be observed if the rotor were to be operated in isolation. The qualitative validity of the data is supported to some extent by the experimental measurements obtained by Lehman[19] which indicate similar thrust settling on the tail rotor of his model helicopter over an equivalent range of flight conditions.

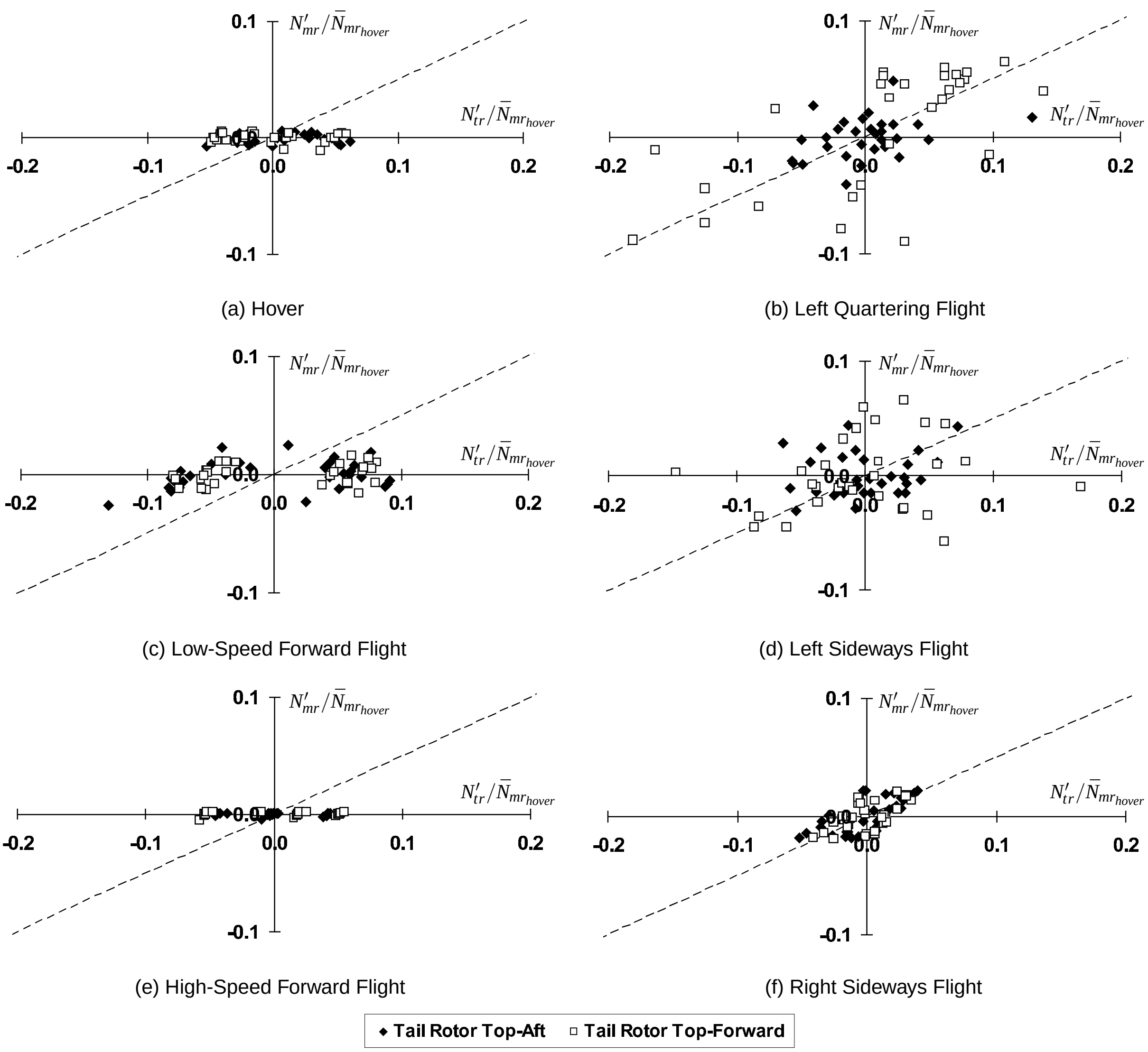

Figure 7: Main and tail rotor contribution to yaw moment

The analytic model given by Newman *et al.*[20] provides a reasonably accurate measure of the speed of onset of the VRS for isolated rotors, and would suggest an advance ratio of about 0.035 for the onset of VRS for the range of thrust coefficients produced by the tail rotor in trimming the aircraft in sideways flight, and about 0.05 for the quartering flight case. These values are supported by calculations for isolated rotors, but are significantly at odds with the results presented in Fig. 8 for the onset of VRS-like behaviour at the tail rotor. It was shown earlier that, even in hover, the development of the tail rotor wake is severely disrupted by interaction with the main rotor, and the results presented here thus raise the question of whether it is appropriate

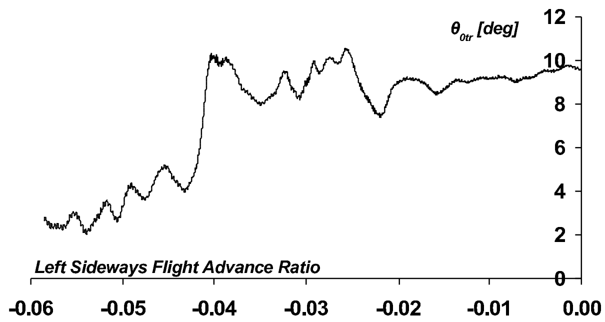

Figure 8: Variation of tail rotor collective pitch in accelerated sideways flight

to analyse the dynamics of the tail rotor using the possibly over-simplified concepts of isolated rotor VRS, or whether instead a more coherent view, spanning a broader range of flight conditions, is required of the disruption of the tail rotor wake that is brought on in the presence of the main rotor. This question is one of those investigated further in the next section of the paper.

5 WAKE INTERACTION

The information presented in the previous section of this paper suggests that the form of aerodynamic interaction responsible for the observed aerodynamic behaviour of the coupled main rotor - tail rotor system may be quite strongly dependent on flight condition. In forward flight, the interaction appears to be dominated by the influence of the main rotor on the tail rotor, whereas the behaviour of the loading in flight conditions with some lateral component of velocity seems to be more strongly influenced by the mutual effect of both rotors on each other. Indeed, it is possible to imagine two rather different modes of aerodynamic interaction taking place within the system. The first, rather obvious ‘direct’ mode would involve the direct impingement of the wake of one of the rotors on the other, and thus a direct and strong modification of the aerodynamic environment experienced by the blades and hence the performance of the affected rotor. The second ‘indirect’ mode, where interaction between the wakes of the rotors - perhaps even at quite some distance from the rotors themselves - modifies the geometry of both wakes, and thus feeds back into the aerodynamic environment of the system and hence the loading on the rotors in a far more subtle way than in the first case, has not received much attention in the past.

The possible existence of the direct mode of interaction can be reasonably clearly inferred from an examination of the mean geometry of the wake, whereas the existence of the second, indirect mode requires a somewhat more tenuous extrapolation from an analysis of local fluctuations in the strength of the wake to determine the locations of the regions of maximum aerodynamic unsteadiness in the system. Figs. 10 and 11 show the wakes generated by the system under the various flight conditions discussed previously. In each figure, the diagram at left shows an illustrative snapshot of the wake structure at one particular instant during its evolution while the figure at right shows the wake decomposed into a relatively steady, mean component (light, translucent surface) and a fluctuating component (dark surface) by applying the analysis presented in Section 3 to simulated wake data collected over several rotor revolutions.

Comparison of Figs. 3(c), 9 and 10(a) reveals the changes in wake structure as the forward speed of the helicopter is increased. Since the tip speed for both main and tail rotors is very similar for the configuration tested here, the wakes of both rotors in isolation behave very similarly at the same forward speed. As the advance ratio of the system is increased, the cylindrical, hover-like wake of the isolated rotor skews back and the vorticity begins to roll up shortly behind the rotor disc, eventually to form a pair of concentrated, counter-rotating 'super- vortices' along either side of the wake. At an advance ratio of about 0.1, the wake of an isolated rotor undergoes a transition from the tubular form found at lower advance ratio to a flattened, more aeroplane-like form. As the forward speed of the rotor is increased, the structure of the wake becomes more pronounced, and the point of visible disruption of the wake as a result of the inherent instability of its vortical structure moves further and further downstream of the rotor. This isolated rotor-like behaviour is still evident in the geometries of the wakes of the coupled main rotor - tail rotor system. For instance, the transition in the form of the wakes of both main and tail rotors is very clear when comparing the flow fields shown in Figs. 9 ($\mu = 0.16$) and 10(a) ($\mu = 0.04$). The situation is complicated though by the increasing impingement of the main rotor wake on the tail rotor as the forward speed is increased. In the low-speed forward flight case, although roughly the bottom quarter of the tail rotor is immersed in the wake of the main rotor, the tail rotor wake maintains its tubular form for quite some distance before gradually merging with the main rotor wake some 3-4 main rotor radii downstream of the rotors. In the high-speed forward flight case, whilst the entire lower half of the tail rotor is immersed in the wake of the main rotor, the distinct character of the tail rotor wake is visible as the spine-like feature that persists for well over twelve main rotor radii down the centre of the wake of the combined system.

It was shown earlier that of the two forward flight cases, the greatest fluctuations in the performance of the system were to be found in the low-speed forward flight case. The degree of direct impingement of the main rotor wake on the tail rotor cannot thus be the prime factor in governing the low-frequency unsteadiness in the forces produced by the system. Fig. 10(b), showing the decomposition of the wake into persistent and fluctuating components in low-speed forward flight, unsurprisingly shows a significant zone of unsteadiness around which the main rotor wake impinges on the tail rotor. This unsteadiness is, in all likelihood, directly responsible for the unsteadiness in the loads generated by the tail rotor. Importantly though, the unsteadiness in the wake also extends outwards in a crescent shaped arc along the trajectory followed by the lower super-vortex from the tail rotor as it merges into the wake of the main rotor. Comparison of Fig. 10(b) with Fig. 10(d) demonstrates that the shape of this arc is subtly dependent on the direction of tail rotor rotation. The secondary region of strong unsteadiness in the super-vortex on the advancing side of the main rotor wake in this flight conditions is probably not related to the interaction between the two rotors, but this unsteadiness and the excitation of the retreating side super-vortex by the tail rotor wake may both be partially responsible for indirectly forcing the rather weak unsteadiness in the loading on the main rotor that is observed in this flight condition.

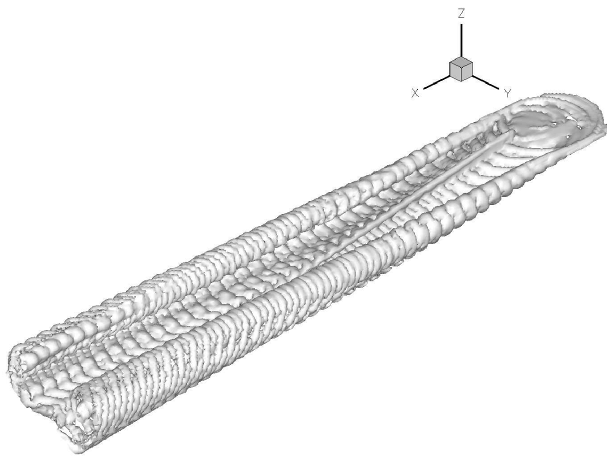

Figure 9: Wake of main rotor - tail rotor system in high-speed forward flight (tail rotor rotating top-aft).

In the quartering flight case, the tail rotor is located upwind of the main rotor, and the free stream thus aids in the tail rotor wake being entrained almost directly into the wake of the main rotor where it causes significant disruption to the development of the leading edge of the main rotor wake. This disruption is clearly evident in the snapshots presented in Figs. 10(e) and 10(g) and appears in the associated decompositions of the wake structure (Figs. 10(f) and 10(h)) as a distinct concentration of the variability in the wake structure down the forward surface of the wake that extends well into the flow downstream of the system. The vorticity distribution surrounding the tail rotor is also highly variable, but, comparing snapshots, the stream of vorticity produced by this rotor appears to be more coherent in structure than in left sideways flight. The direction of rotation of the tail rotor appears to have a rather subtle influence on the distribution of unsteadiness in the wake, but, rather surprisingly, a marked influence on the geometry of the mean wake of the system. A comparison of Figs. 10(f) and 10(h) shows the mean wake of the system with TA tail rotor rotation to be broader and flatter than the wake of the system with tail rotor rotating TF, and this appears be associated, in, admittedly, a rather obscure way, with the induction of the tail rotor wake into the super-vortex on the closest side of the main rotor disc. The principal effect of tail rotor rotation in this flight condition may thus be to promote an indirect mode of interaction between the rotors by raising the fluctuating vorticity field embedded within this super-vortex closer to the main rotor disc, where it can have a greater effect on the unsteadiness of the loads produced by the system.

It is highly instructive to compare the wake geometries generated by the rotors in left-sidewards and right-sidewards flight. In right sidewards flight (Fig. 11(e)-11(h)), the effect of the free-stream in having a significant component in the direction of the induced velocity of the tail rotor is to prevent the wake tube produced by the tail rotor from being entrained through the main rotor. Instead, the wake tube remains relatively intact as it extends a considerable distance downstream, parallel to the super-vortex on the same side of the main rotor disc. The induced velocity field of the super-vortex gradually flattens the tail rotor wake tube and bends it slightly inwards towards the centre-line of the main rotor wake, and eventually the two wakes merge within the highly disrupted flow well downstream of the rotors. This fairly ordered structure produces very isolated and small regions of fluctuation in the wake, consistently with the low levels of fluctuating load observed under this flight condition. In contrast, the left-sidewards flight case (Figs. 11(a)-11(d)) is much more interesting since the free stream velocity, now in opposition to the induced velocity of the tail rotor, prevents the tail rotor wake from advancing very far downstream. Instead it is drawn towards the main rotor, and parts of the tail rotor wake tube are subsequently entrained into the main rotor wake in a highly unsteady process that extends back to the tail rotor disc. This dynamics is most likely the direct cause of the fluctuations in loading observed on the tail rotor. Those remnants of the tail rotor wake that are not ingested into the main rotor are emitted in highly disrupted form as a stream of fragments that are convected back into the wake behind the system along a trajectory that is almost the mirror image of that of the tail rotor wake in right sidewards flight. As in right sidewards flight, the induced velocity field of the super-vortex on the closest side of the main rotor flattens this stream of vorticity and rotates it inboard causing it to interact rather strongly with the periphery of the main rotor near the point of formation of the super-vortex. Given the highly unsteady nature of the stream of vorticity emanating from the tail rotor, this interaction has a significant effect in increasing the unsteadiness of the flow in the super-vortex itself, and the presence of this indirect mode of interaction is the most likely cause of the substantially increased unsteadiness in the loading produced by the main rotor in left sidewards flight compared to right sidewards flight. The effect of tail rotor sense of rotation is not immediately obvious, however, since Figs. 11(b) and 11(d) show a change in direction of rotation of the tail rotor to be accompanied by no gross changes in the structure of the mean wake, and only subtle shifts in location of the regions of major unsteadiness within the flow field of the system.

Returning to the question of whether or not the tail rotor exhibits vortex ring-like behaviour in left sideways and quartering flight, comparison of Figs. 11(a) and 10(e) (the hover wake shown in Fig. 3 can be included as a useful intermediate case) shows that the behaviour of the flow near the tail rotor in lateral flight does not really exhibit the classical VRS onset mechanism of a fairly abrupt breakdown of a cylindrical wake tube into a toroidal form, over a small range of free-stream velocities that oppose the induced flow through the rotor, as in the case of an isolated rotor. The simulations suggest instead that the tail rotor wake is highly disrupted in all lateral flight conditions by its entrainment into the wake of the main rotor. Indeed, the principal mode of behaviour of the tail rotor wake, in response to a change in the component of the free stream that is parallel to its axis, appears simply to be a lengthening or shortening of the segment of the wake tube that is left relatively undisturbed by this entrainment. The reason why the response of the rotor does appear to have a vortex ring like character at the highest opposing free stream velocities can be inferred with reasonable confidence from the figures: under these conditions the undisturbed segment of the wake does indeed become very short, and the tail rotor itself thus becomes immersed in the highly unsteady vorticity field associated with the entrainment of the tail rotor vorticity into the wake of the main rotor. Thus the wake of the combined system does indeed bear some of the hallmarks of the flow field generated by an isolated rotor immersed in the classical VRS, and it is not surprising that the tail rotor exhibits similar performance characteristics under these conditions.

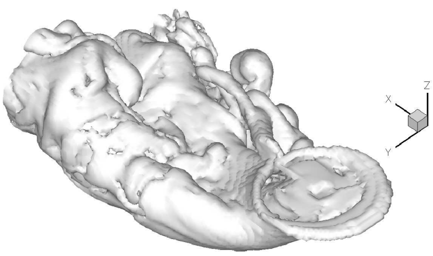

(a) Forward flight TA, instantaneous

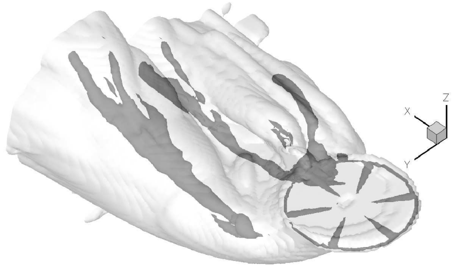

(b) Forward flight TA, mean and RMS

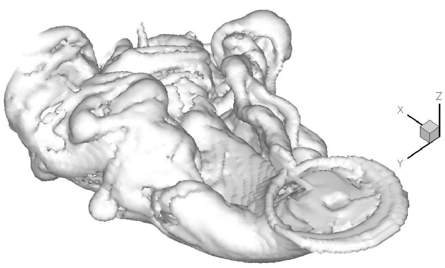

(c) Forward flight TF, instantaneous

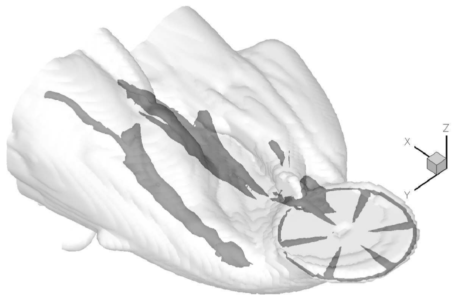

(d) Forward flight TF, mean and RMS

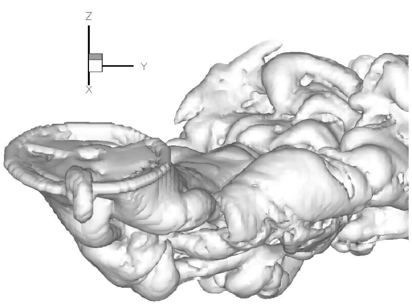

(e) Quartering flight TA, instantaneous

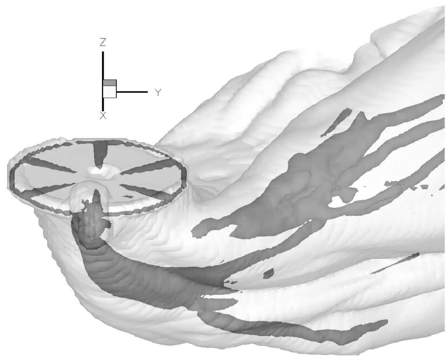

(f) Quartering flight TA, mean and RMS

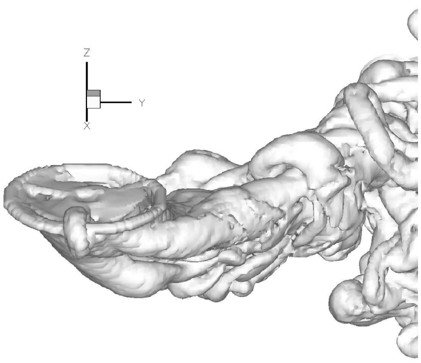

(g) Quartering flight TF, instantaneous

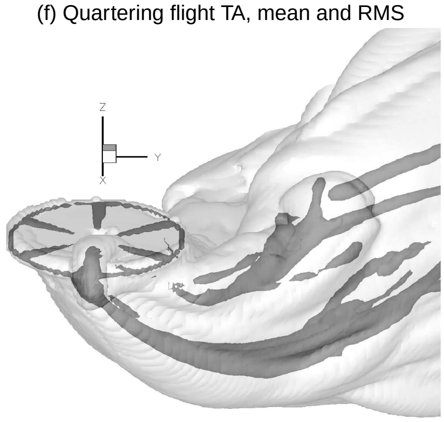

(h) Quartering flight TF, mean and RMS

Figure 10: Wake structure in various flight conditions

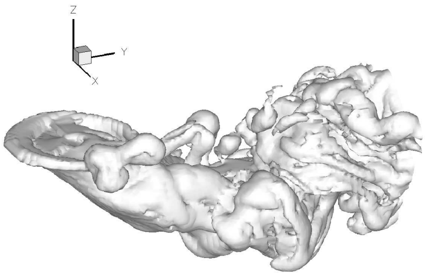

(a) Left Sideways flight TA, instantaneous

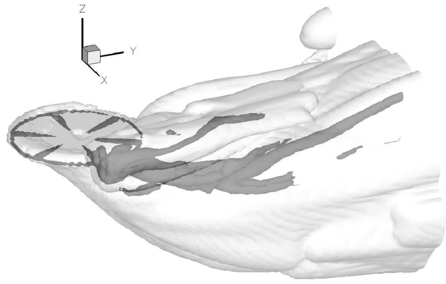

(b) Left sideways flight TA, mean and RMS

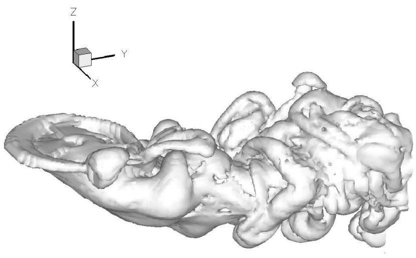

(c) Left sideways flight TF, instantaneous

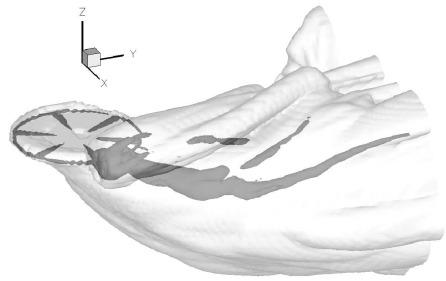

(d) Left sideways flight TF, mean and RMS

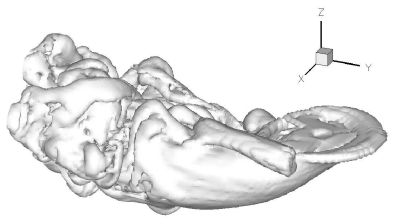

(e) Right sideways flight TA, instantaneous

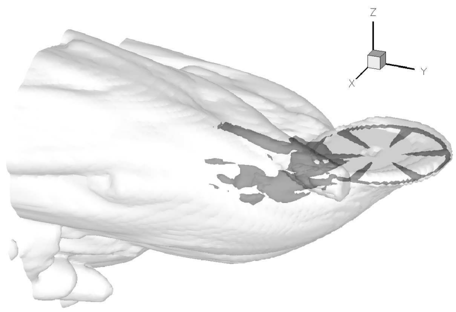

(f) Right sideways flight TA, mean and RMS

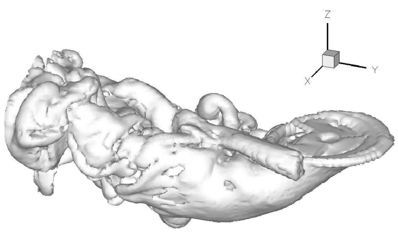

(g) Right sideways flight TF, instantaneous

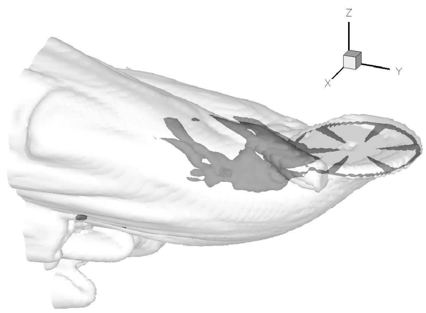

(h) Right Sideways flight TF, mean and RMS

Figure 11: Wake structure in various flight conditions

6 IMPLICATIONS FOR HELICOPTER DIRECTIONAL CONTROL

To place the data presented in this paper in perspective, it is useful to bear in mind that one degree of tail rotor collective pitch input would require roughly six to seven percent of the pedal travel available to the pilot on a typical helicopter. This implies that the three degrees or so maximum variation in collective pitch observed in the worst cases presented in Fig. 6 would correspond to pedal motion over roughly twenty percent of the available range. Furthermore, the data presented in Fig. 6 shows that the largest-amplitude variations in tail rotor collective pitch would be required to be made with a characteristic period of roughly 5-10 main rotor revolutions. For a typical helicopter, where the main rotor might rotate at a frequency of 4-5Hz, the largest control applications would thus be required at a frequency in the range of 0.5-1Hz. This combination of amplitude and frequency of pedal input would arguably be manageable, but nevertheless extremely distracting and tiresome for the pilot under even the most benign operational conditions. Note too that if the pilot were tempted to remain passive rather than to actively apply the requisite control inputs to trim the aircraft, excitation of the system in the 0.5-1Hz frequency range would stimulate the yaw dynamics of the airframe, quite possibly resulting in a rather objectionable lateral oscillation of the system.

In applying the results presented in this paper to the real situation, however, the implications of some of the simplifications that were embodied in the analysis, here simply for the purposes of better understanding the aerodynamic effects that govern the interaction between the main and tail rotors, should be borne firmly in mind. Whilst the yaw dynamics of the helicopter may indeed be excited by fluctuations in the yaw moment produced by the rotors, as observed here, the role of the fuselage, tail boom and empennage in acting as strong modifiers to the dynamics of the isolated rotors needs also to be considered. Although the main and tail rotors might be the principal sources of the forces and moments exerted on the helicopter, the loads developed on the fuselage and fin can also be significant. Their contributions to the yaw moment of the aircraft, both as a result of sideslip and yaw rate, may be expected to modify quite strongly the control inputs required at the tail rotor to maintain the yaw equilibrium of the system in any particular flight condition. A lateral dynamic which is suppressed by the very changes to the forces and moments on the helicopter that it induces may be of little consequence to the handling qualities of the vehicle. Conversely, though, one which leads to a divergence in yaw attitude may be highly problematic. Further insight here will require the use of a model that is capable of capturing both the yawing motion of the airframe and the dynamic nature of the resultant flow field that surrounds te helicopter. Of course, the fuselage, fins and other components of the airframe act themselves to modify the aerodynamic environment experienced by the rotors. As such, the aerodynamic mechanisms postulated here as the underlying factors governing the interaction between the main and tail rotors may be overwhelmed, in certain cases, by certain configuration-specific elements of the flow field. In such conditions, one may only conjecture as to the specific characteristics of the lateral response of the aircraft, and a generic analysis such as presented here may not be of much specific use. It is particularly these configuration-specific issues that will provide industrial CFD practitioners with a rich source of employment for many years to come, but it is hoped that more general analyses such as the one presented here will be of assistance in providing the fundamental framework within which the more case-specific features of the aerodynamic interaction between the main and tail rotor of any particular configuration can be analysed and understood.

7 CONCLUSION

Simulations of an idealised helicopter, consisting of a main and tail rotor arranged in conventional configuration, have been performed in a range of flight conditions including hover, low-speed and high-speed forward flight, and three conditions with a lateral component of velocity. The helicopter was modelled as an isolated pair of rotors to avoid other physical factors from obscuring the effects of the aerodynamic interaction between the wakes of the two rotors on the loads produced within the system. Previous studies have suggested that the flight condition as well as the direction of tail rotor rotation (top-forward or top-aft) has a significant effect, particularly on the unsteadiness of the forces produced by the tail rotor. The numerical data presented in this paper support these observations, and the detailed flow-field information that is available from the simulations allows some insight into the aerodynamic effects that are responsible for the unsteadiness in the system.

In particular, simulations show distinct differences in the behaviour of the system in left sidewards and right sidewards flight that are consistent with flight experience that the greatest fluctuations in loading or conrol input are required in left sideways flight (for a counter-clockwise rotating rotor) and are generally more extreme for a system with tail rotor rotating top-forward than top-aft. The simulations also expose distinct differences in the character of the lateral excitation of the system as forward flight speed is varied, and suggest the existence of an intermediate flight speed at which the lateral dynamics of the system is most strongly affected by fluctuations in the loads on the system. Traces of very low-frequency periodicity in the simulated results at low forward speed may be evidence that main rotor - tail rotor interaction may be partially responsible for such practically-encountered lateral oscillations such as tail shake or lateral snaking but further investigation, involving significantly longer computational runs than attempted here, is warranted before definite conclusions can be drawn.

The key aerodynamic factor that helps to explain all the cases presented here, though, appears to be the fact that the tail rotor wake undergoes a distinct change in geometry when exposed to the flow-field of the main rotor. Instead of streaming out laterally as a coherent tube, as it would in isolation from the main rotor, the wake is disrupted downstream of the tail rotor by a process whereby some or all of its vorticity is entrained into the wake of the main rotor. This entrainment is in all cases a highly unsteady process, and the degree of unsteadiness appears to depend, to some extent, on the direction of rotation of the tail rotor. The disruption to rotor loading appears to be strongly linked to the proximity of the major regions of entrainment-related unsteadiness in the combined wake of the main-tail rotor system to the rotor in question. In high-speed forward flight and right sidewards flight, the free stream acts to delay the entrainment to far enough downstream of the system for the perturbations to the rotor loading to be slight. Conversely though, in left sidewards and quartering flight, the action of the free stream is to confine the entrainment process very close to the rotors where it has a major effect on the unsteadiness of the loads produced by the system.

As is often the case in as complex a set of flows as this, though, the direct link between cause and effect remains tenuous, and in some cases even elusive. Much further work needs to be done to understand the detailed effects of the aerodynamic interactions that occur in the flow around the closely-coupled main rotor - tail rotor geometry of the conventional helicopter configuration on the loads that are produced. Nevertheless, the results of the case study presented here demonstrate that current computational models are indeed sensitive to important operational factors, such as the flight condition of the helicopter, as well as to the more detailed, specific features of the helicopter configuration such as the direction of rotation of the tail rotor that are known to influence the interactional aerodynamic environment of the helicopter. This bodes well for our future understanding of the extremely complex aerodynamics that underlies the performance of the various closely-coupled components of the helicopter system.

ACKNOWLEDGEMENTS

The research reported in this paper has been made possible through the support and sponsorship of the U.S. Government through its European Research Office of the U.S. Army.

REFERENCES

1. Sheridan, P.F., and Smith, R.P., “Interactional Aerodynamics - A New Challenge to Helicopter Technology,” *Journal of the American Helicopter Society*, Vol. 25, No. 1, 1980, pp. 3-21.

2. Lynn, R.R., Robinson, F.D., Batra, N.N., and Duhon, J.M., “Tail Rotor Design Part 1: Aerodynamics,” *Journal of the American Helicopter Society*, Vol. 15, No. 4, 1970, pp. 2-15.

3. Johnston, J.F., and Cook, J.R., “AH-56A Vehicle Development,” 27th Annual Forum of the American Helicopter Society, Washington D.C., USA, 1971.

4. Amer, K.B., Prouty, R.W., Walton, R.P., and Engle, J.E., “Handling Qualities of Army/Hughes YAH-64 Advanced Attack Helicopter,” 34th Annual Forum of the American Helicopter Society, Washington D.C., USA, 1978, pp.78.31.1-78.31.17.

5. Prouty, R.W., “Helicopter Performance, Stability, and Control,” Robert E. Krieger Publishing, Florida, USA, 1986, pp. 107-111.

6. Yeager, W.T., Jr, Young, W.H., Jr, and Mantay, W.R., “A Wind-Tunnel Investigation of Parameters Affecting Helicopter Directional Control at Low Speeds in Ground Effect,” NACA TN D-7694, 1974.

7. de Waard, P., and Trouvé, M., “Tail Shake Vibration in Flight: Objective Comparison of Aerodynamic Configurations in a Subjective Environment,” 55th Annual Forum of the American Helicopter Society, Montreal, Canada, 1999.

8. Balch, D.T., “Experimental Study of Main Rotor/Tail Rotor/Airframe Interaction in Hover,” 39th Annual Forum of the American Helicopter Society, St. Louis, Missouri, USA, 1983.

9. Empey, R.W., and Ormiston, R.A., “Tail-Rotor Thrust on a 5.5-foot Helicopter Model in Ground Effect,” 30th Annual National Forum of the American Helicopter Society, 1974, pp. 1-13.

10. Wiesner, W., and Kohler, G., “Tail Rotor Performance in Presence of Main Rotor, Ground, and Winds,” *Journal of the American Helicopter Society*, Vol. 19, No. 3, 1974, pp. 2-9.

11. Brocklehurst, A., *personal communication*.

12. Brown, R.E., “Rotor Wake Modelling for Flight Dynamic Simulation of Helicopters,” *AIAA Journal*, Vol. 38, No. 1, 2000, pp. 57-63.

13. Brown, R.E., and Line, A.J., “Efficient High-Resolution Wake Modelling using the Vorticity Transport Equation,” *AIAA Journal*, Vol. 43, No. 7, 2005, pp. 1434-1443.

14. Toro, E.F, “A Weighted Average Flux Method for Hyperbolic Conservation Laws,” *Proceedings of the Royal Society of London, Series A: Mathematical and Physical Sciences*, Vol. 423, No. 1864, 1989, pp. 401-418.

15. Brown, R.E., and Houston, S.S., “Comparison of Induced Velocity Models for Helicopter Flight Mechanics,” *Journal of Aircraft*, Vol. 37, No. 4, 2000, pp. 623-629.

16. Houston, S.S., and Brown, R.E., “Rotor-Wake Modeling for Simulation of Helicopter Flight Mechanics in Autorotation,” *Journal of Aircraft*, Vol. 40, No. 5, 2003, pp. 938-945.

17. Whitehouse, G.R., and Brown, R.E., “Modeling the Mutual Distortions of Interacting Helicopter and Aircraft Wakes,” *Journal of Aircraft*, Vol. 40, No. 3, 2003, pp. 440-449.

18. Brown, R.E., Leishman, J.G., Newman, S.J., and Perry, F.J., “Blade Twist Effects on Rotor Behaviour in the Vortex Ring State,” Cheeseman Award Lecture, 59th Annual Forum of the American Helicopter Society, Phoenix, Arizona, 2003.

19. Lehman, A.F., “Model Studies of Helicopter Tail Rotor Flow Patterns In and Out of Ground Effect,” USAAVLABS TR 71-12, 1971.

20. Newman, S.J., Brown, R., Perry, F.J., Lewis, S., Orchard, M., and Mohda, A., “Predicting the Onset of Wake Breakdown for Rotors in Descending Flight,” *Journal of the American Helicopter Society*, Vol. 48, No. 1, 2003, pp. 28-38